J Comput Aided Mol Des (2007) 21:499–509
DOI 10.1007/s10822-007-9131-1

Analysis of the activation mechanism of the guinea-pig Histamine H_1-receptor

Andrea Straßer · Hans-Joachim Wittmann

Received: 23 May 2007 / Accepted: 6 August 2007 / Published online: 22 August 2007

Abstract The Histamine H_1-receptor (H_1R), belonging to the amine receptor-class of family A of the G-protein coupled receptors (GPCRs) gets activated by agonists. The consequence is a conformational change of the receptor, which may involve the binding-pocket. So, for a good prediction of the binding-mode of an agonist, it is necessary to have knowledge about these conformational changes. Meanwhile some experimental data about the structural changes of GPCRs during activation exist. Based on homology modeling of the guinea-pig H_1R (gpH_1R), using the crystal structure of bovine rhodopsin as template, we performed several MD simulations with distance restraints in order to get an inactive and an active structure of the gpH_1R. The calculations led to a $Phe^{6.44}$/$Trp^{6.48}$/$Phe^{6.52}$-switch and linearization of the proline kinked transmembrane helix VI during receptor activation. Our calculations showed that the $Trp^{6.48}$/$Phe^{6.52}$-switch induces a conformational change in $Phe^{6.44}$, which slides between transmembrane helices III and VI. Additionally we observed a hydrogen bond interaction of $Ser^{3.39}$ with $Asn^{7.45}$ in the inactive gpH_1R, but because of a counterclockwise rotation of transmembrane helix III $Ser^{3.39}$ establishes a water-mediated hydrogen bond to $Asp^{2.50}$ in the active gpH_1R. Additionally we simulated a possible mechanism for receptor activation with a modified *LigPath*-algorithm.

A. Straßer (✉)
Department of Pharmaceutical and Medicinal Chemistry, Faculty of Chemistry and Pharmacy, University of Regensburg, Regensburg, Germany
e-mail: andrea.strasser@chemie.uni-regensburg.de

H.-J. Wittmann
EDV-Referent, Faculty of Chemistry and Pharmacy, University of Regensburg, Regensburg, Germany

Keywords Guinea-pig Histamine H_1-receptor · G-protein-coupled receptor · Inactive conformation · Active conformation · *LigPath*

Introduction

For G-protein coupled receptors (GPCRs) a crystal structure neither of the inactive state nor of the active state is available up to now. Only crystal structures of bovine rhodopsin are known. To be able to model several GPCRs despite of the lack of their crystal structure the technique of homology modelling is widely accepted [1, 2]. This modelling is based on structural similarity between the structures of GPCRs and bovine rhodopsin. Ballesteros et al. [3] gave an overview over those amino acids which are highly conserved within the transmembrane helices of GPCRs. So the crystal structure of bovine rhodopsin can be used as a template structure. It is clear that the technique of homology modelling mentioned above is an approximation, but up to now nearly no other technique is known to predict the structure [4] of GPCRs. For refinement and improvement of the resulting homology models it is state of the art to embed the GPCR in its surrounding like lipid bilayer and water and to carry out molecular dynamics simulations. The structure, as result of homology modelling represents the inactive conformation of the receptor. It is proposed that agonists induce a conformational change of the GPCRs during receptor activation [5–19], which may result in a different structure of the binding-pocket with respect to the inactive state. Using an inactive receptor model for modeling agonists in the binding-pocket may result in problems concerning optimal docking of the ligand. So it is advantageous to have an active receptor model. In the last years, several experimental techniques

like site-directed spin labelling [20, 21], fluorescence quenching [22] and nuclear magnetic resonance spectroscopy [23] were used to achieve information about the active conformation of bovine rhodopsin and other GPCRs. These results can be used for a constrained homology modeling of the active state. It should be clear that the conclusion by analogy from the active bovine rhodopsin conformation to other GPCRs is an approximation, but up to now no better technique for modelling the active state is available. Niv et al. [24] gave a very good summary about the structural properties of inactive and active bovine rhodopsin and other GPCRs. During the activation process the intracellular part of transmembrane helix (TM) VI moves away from the intracellular part of TM III, that means, the ionic lock between $Arg^{3.50}$ and $Gln^{6.30}$ is destroyed [25–32]. This movement results in a straightening of TM VI. It is suggested that a $Trp^{6.48}$/$Phe^{6.52}$ rotamer toggle switch induces this helix movement [5, 10, 12, 13]. Additionally the mentioned transmembrane helices are proposed to rotate counterclockwise [7, 8]. Highly conserved internal water molecules seem to be involved in receptor activation according to Pardo et al. [33].

Based on these data our aim was to model not only the inactive and active state of the guinea-pig Histamine H_1 receptor (gpH_1R) but also intermediate states of the gpH_1R during its activation and to achieve information about the activation mechanism to get information suitable for future prediction of agonism or antagonism of an arbitrary ligand. In cooperation with Seifert [34] we showed with the help of steady state GTPase assay experiments, that the gpH_1R is constitutive active to a small extent. That means that a distinct amount of the gpH_1Rs is present in its active conformation without the presence of an agonist. So we will perform calculations without any agonist in this work.

Methods

Numbering of residues, nomenclature of χ_1 rotamer and the *rmsd*

The residues are numbered relative to the most conserved residues in the transmembrane helix according to Ballesteros et al. [3]. The torsion angle χ_1 is calculated in the following manner: For a given chain X–A–B–Y the torsion angle χ_1 is defined as the angle between the orthogonal projections of the bonds X–A and B–Y into the plane bisecting the bond A–B, when viewed from A to B. The angle is considered positive, if the bond in front of the bisecting plane has to be rotated in a clockwise manner to eclipse the bond behind the bisecting plane. We use the following assignment: X = N, A = C_α, B = C_β and Y = C_γ. The root mean square distance *rmsd* of each receptor state *s* (inactive or each state between inactive and active) with respect to the active state of the receptor is defined as given in Eq. 1.

$$rmsd = \sqrt{\frac{\sum_{i=1}^{N}\left(\left(x_s^i - x_{active}^i\right)^2 + \left(y_s^i - y_{active}^i\right)^2 + \left(z_s^i - z_{active}^i\right)^2\right)}{N}} \quad (1)$$

The *rmsd* is calculated including all *N* receptor atoms with the coordinates (x_s^i, y_s^i, z_s^i) for atom *i* in the state *s* and the coordinates (x_{active}^i, y_{active}^i, z_{active}^i) for atom *i* in the active state.

Construction of a receptor model in a simulation box and force field parameters

The gpH_1R model was constructed, as described in [35] using the software SYBYL 7.0 [36] and VEGA ZZ [37], based on the 3D-crystal structure of bovine rhodopsin (1F88) [38, 39]: the homology between the gpH_1R and bovine rhodopsin after sequence alignment (see [35]) is about 20% with respect to the transmembrane domains, if also very similar amino acids are considered, the homology is about 32%. Additionally we included the conserved internal water molecules in our receptor model using the crystal structure 1GZM [38, 40] of bovine rhodopsin, since the internal water molecules might be involved in GPCR stabilization or activation [33]. For a more realistic model we also included the surrounding of the gpH_1R: First we embedded the receptor in a POPC membrane bilayer (104 molecules) manually with the help of the software package VEGA [37]. Afterwards we filled the whole simulation box (7.473 nm × 7.64 nm × 10.5 nm) with SPC water molecules using GROMACS 3.2 [41]. To achieve electroneutrality we placed an appropriate number of eight sodium and 25 chloride ions into the box. Finally the simulation box contained 12,675 water molecules. For all calculations the software package GROMACS 3.2 [41] with the ffG53A6 force field [42] was used. All calculations were performed with the following GROMACS [41] parameters concerning energetics: coulombtype = PME, rcoulomb = 1.4, epsilon_r = 1.0, vdw_type = Cut-off, rvdw = 1.4 and DispCorr = EnerPress. For visualization we used vmd [43, 44].

Modeling of the inactive and active receptor

The gpH_1R model, directly based on homology modeling, is an inactive receptor model. Though the model was

energy minimized, the hydrogen bonding network between the amino acid side chains is perhaps not optimal yet. Because of that the inactive conformation of the gpH_1R was refined with a distance-restrained MD-Simulation, using the constraints for the inactive conformation given in Niv et al. [24]. The active model of the gpH_1R was also generated with a distance-restrained MD-Simulation, based on the constraints for the active conformation given by Niv et al. [24]. The original as well as slightly modified constraints for $Phe^{6.52}$ and $Trp^{6.48}$, which we have applied in this work, are given in Table 1. Besides that, we applied distance restraints for the hydrogen-bonds of the transmembrane helices. The helical distance restraints were introduced between the backbone oxygen of residue (i) and the backbone nitrogen of residue ($i + 4$). The constraints were imposed on the complete transmembrane helices except for the prolines. All simulations was carried out at a temperature of 310 K and were divided into 201 cycles, each which a simulation time of 2 ps. Starting with a force constant of 0 kJ mol^{-1} nm^{-2} in the first cycle, the force constant was raised about 100 kJ mol^{-1} nm^{-2} per cycle until a force constant of 20,000 kJ mol^{-1} nm^{-2} was reached in the last cycle. Following the force constant was reduced in 201 simulation cycles until a force constant of 0 kJ mol^{-1} nm^{-2} was reached. In each of these cycles with a simulation time of 2 ps the force was decreased in steps of 100 kJ mol^{-1} nm^{-2}. After that a period of 100 ps of free simulations followed. In all MD simulations Berendsen temperature and pressure coupling was used. The described procedure is illustrated as flow chart in Fig. 1.

Modification of the *LigPath*-algorithm for approximate calculation of an activation mechanism of the gpH_1R

For approximate calculation of a possible activation mechanism of the gpH_1R we used a modified version of the *LigPath*-algorithm [35]. In the former version described in [35], we only had to define the starting structure of the receptor and/or ligand and the destination structure of the ligand in the binding pocket. In this new version we added the possibility to give the destination coordinates of the receptor as additional input information into the algorithm. During the activation process of a GPCR long range movements of TM VI are described in literature [25–32], which we could not observe entirely in the old version. Therefore we allow the receptor atoms to be translated from their actual position into their destination position on an analogous guiding line as described for the ligand in [35]. To guarantee highest flexibility for the short and long range receptor movement we further allow the receptor atoms a randomly determined deviation within a defined range from the guiding line, which is recalculated for each receptor atom in each child and generation. All other parts of the algorithm were used, as described in [35]. The child with lowest potential energy of the receptor and internal water molecules defines the starting structure for the next generation.

Parameters for approximate calculation of an activation pathway for the gpH_1R with the modified *LigPath*-algorithm

As destination structure for activation and inactivation pathway calculations we used the last structure we got of our MD-Simulations to achieve the inactive and the activate structure of the gpH_1R (Fig. 1). All pathway calculations are carried out without a ligand, but including the whole simulation box (gpH_1R, membrane, solute, ions) and the internal water molecules. We performed several calculations with different input parameters given in Table 2. The rotable bonds of the amino acid side chains are defined, as given in [35]. We calculated the activation pathway as well as the inactivation pathway. For the activation pathway the inactive structure was used as starting structure and the active structure as destination structure, and vice versa for the inactivation pathway. For the minimization steps during the *LigPath* calculation a maximum of 10,000 iterations were allowed to reach a maximum force smaller than 10 kJ mol^{-1} nm^{-1} in the minimization.

Evaluation of the calculated receptor conformations

The quality of the inactive as well as the active gpH_1R structures, as result of the MD simulations were proofed with the help of Ramachandran plots. Additionally we randomly proofed structures of our pathway calculations with the Ramachandran analysis. All tests showed that more than 90% of the amino acids are in the favoured region and less than 4% in the outlier region, which is a well acceptable result.

Results and discussion

The inactive model of the gpH_1R

The time course of the *rmsd* of the whole gpH_1R with respect to the energy minimized homology model during the generation of the inactive state is given in Fig. 2. After 50 ps of simulation time, no significant changes in *rmsd* are observed. The resulting inactive state model of the gpH_1R shows an *rmsd* of 0.182 nm with respect to the starting structure for the MD-Simulation. Interhelical hydrogen

Table 1 Position restraints (between C_α atoms unless indicated otherwise; atom types are given in GROMACS [41] notation) given by Niv et al. [24] and the restraints used in our simulations

No. of restraint	Amino acid 1			Amino acid 2			Inactive (nm), Niv et al. [24]	Inactive (nm), this work	Active (nm), Niv et al. [24]	Active (nm), this work
	No. [3]	Bovine rhodopsin	gpH_1R	No. [3]	Bovine rhodopsin	gpH_1R				
1	1.56	V	A	7.63*	C	T	0.679	0.679	>0.710	0.860
2	1.57	T	V	7.63*	C	T	0.848	0.848	>0.860	0.960
3	1.60	H	E	7.53*	Y	Y	–	–	>1.559	1.570
4	1.60	H	E	7.55*	M	L	–	–	1.795–1.802	–
5	1.60	H	E	7.56*	M	C	–	–	1.796–1.815	–
6	1.60	H	E	7.57*	N	N	–	–	>1.472	1.500
7	1.60	H	E	7.59*	Q	N	–	–	1.066–1.115	1.110
8	1.60	H	E	7.60*	F	F	0.895	0.895	0.930–0.950	–
9	1.60	H	E	7.61*	R	R	–	–	1.181–1.194	–
10	1.60	H	E	7.62*	N	K	–	–	1.092–1.140	1.140
11	1.60	H	E	7.66*	T	R	0.921	0.921	0.943–0.990	0.960
12	2.60	T	M	3.28	E	W	0.469	0.469	0.650–0.850	0.850
13	2.64	T	Y	3.25	C	C	0.824	0.824	0.650–0.850	0.850
14	3.32	A	D	7.39	A	I	0.895	0.895	0.650–0.850	0.850
15	2.38	P	V	7.63*	C	T	–	–	>1.695	1.790
16	2.39	L	G	7.63*	C	T	–	–	>1.469	1.730
17	3.50	R	R	6.32	E	K	–	–	>1.800	2.200
18	3.50	R	R	6.34	T	A	0.655	0.655	>1.800	1.810
19	3.51	Y	Y	5.57	C	F	0.553	0.553	>0.800	0.880
20	3.51	Y	Y	5.60	Q	R	0.665	0.665	<0.800	0.800
21	3.53	V	S	6.30	E	E	0.694	0.694	>0.850	2.000
22	3.53	V	S	6.31	K	R	–	–	>0.850	2.600
23	3.53	V	S	6.32	E	K	–	–	>0.850	2.600
24	3.53	V	S	6.33	V	A	0.837	0.837	>0.850	2.080
25	3.53	V	S	6.34	T	A	0.926	0.926	>0.850	2.290
26	3.53	V	S	6.35	R	K	–	–	>0.850	2.600
27	3.54	V	V	6.30	E	E	0.759	0.759	>1.800	2.080
28	3.54	V	V	6.31	K	R	0.919	0.919	>1.800	2.360
29	3.54	V	V	6.32	E	K	–	–	>1.800	2.570
30	3.54	V	V	6.33	V	A	–	–	>1.800	2.250
31	3.54	V	V	6.34	T	A	0.894	0.894	>1.800	2.250
32	3.55	C	Q	5.57	C	F	0.953	0.953	>0.800	1.190
33	3.55	C	Q	5.60	Q	R	0.747	0.747	<0.800	0.800
34	5.35	N	V	6.59	F	A	–	–	<0.800	0.800
35	5.39	V	K	6.59	F	A	0.820	0.820	<0.800	0.800
36	5.62	V	Y	6.34	T	A	–	–	0.876	0.870
37	5.62	V	Y	6.35	R	K	–	–	<0.935	0.940
38	5.62	V	Y	6.36	M	Q	–	–	<1.267	1.260
39	5.63	F	K	6.27	L	M	–	–	<1.156	1.156
40	3.36	G	S	6.48	W	W	0.831	–	>0.550	–
41	3.36	G	S	6.48 (CB)	W	W	0.707	–	>0.550	–
42	3.36	G	S	6.48 (CG)	W	W	0.579	–	>0.550	–
43	3.36	G	S	6.48 (CD1)	W	W	0.529	–	>0.550	–
44	3.36	G	S	6.48 (CD2)	W	W	0.534	–	>0.550	–
45	3.36	G	S	6.48 (CE2)	W	W	0.444	–	>0.550	–
46	3.36	G	S	6.48 (CE3)	W	W	0.601	–	>0.550	–

Table 1 continued

No. of restraint	Amino acid 1			Amino acid 2			Inactive (nm), Niv et al. [24]	Inactive (nm), this work	Active (nm), Niv et al. [24]	Active (nm), this work
	No. [3]	Bovine rhodopsin	gpH_1R	No. [3]	Bovine rhodopsin	gpH_1R				
47	3.36	G	S	6.48 (CZ2)	W	W	0.413	–	>0.550	–
48	3.36	G	S	6.48 (CZ3)	W	W	0.577	–	>0.550	–
49	3.36	G	S	6.48 (CH2)	W	W	0.491	–	>0.550	–
40**	6.48 (O)	W	W	6.48 (CG)	W	W	–	–	–	0.289
41**	6.48 (O)	W	W	6.48 (CD1)	W	W	–	–	–	0.350
42**	6.48 (O)	W	W	6.48 (CD2)	W	W	–	–	–	0.284
43**	6.48 (O)	W	W	6.48 (CE2)	W	W	–	–	–	0.345
44**	6.48 (O)	W	W	6.48 (CE3)	W	W	–	–	–	0.322
45**	6.48 (O)	W	W	6.48 (CZ2)	W	W	–	–	–	0.423
46**	6.48 (O)	W	W	6.48 (CZ3)	W	W	–	–	–	0.404
47**	6.48 (O)	W	W	6.48 (CH2)	W	W	–	–	–	0.450
48**	6.52 (N)	A	F	6.52 (CG)	A	F	–	–	–	0.387
49**	6.52 (N)	A	F	6.52 (CD1)	A	F	–	–	–	0.481
50**	6.52 (N)	A	F	6.52 (CD2)	A	F	–	–	–	0.455
51**	6.52 (N)	A	F	6.52 (CE1)	A	F	–	–	–	0.608
52**	6.52 (N)	A	F	6.52 (CE2)	A	F	–	–	–	0.587
53**	6.52 (N)	A	F	6.52 (CZ)	A	F	–	–	–	0.653

*: constraints beyond amino acids of the C-terminus are numbered subsequently concerning the numbering scheme for TM VII; **: constraints 40**–47** adequate to constraints from Niv et al. [24], but different reference point, constraints 49**–53** introduced in this work

bonds between the transmembrane helices were detected as given in Table 3.

The active model of the gpH_1R

Additionally in Fig. 2 the time course of the *rmsd* during generation of the active state of the gpH_1R, starting with the energy minimized homology model is shown. After 300 ps of simulation time, no significant changes in *rmsd* are observed. The active state model of the gpH_1R shows an *rmsd* of 0.472 nm with respect to the homology model, and an *rmsd* of 0.448 nm with respect to the inactive state. The two branches of the proline kinked TM VI form an angle denoted by α, which was straightened from about 135° in the inactive state to 150° in the active state (Fig. 3). A full straightening to 180° was not reached with the constraints applied. The $Trp^{6.48}/Phe^{6.52}$—switch (Fig. 3) could only be observed, when using our referring constraints (no. 40**–53**), as given in Table 1 but not with the original constraints given from Niv et al. [24]. But a conformational change of $Phe^{6.44}$ resulted in our calculations, without any constraints on this side chain. In the inactive state $Phe^{6.44}$ forms an aromatic cluster with $Trp^{6.48}/Phe^{6.52}$, which undergoes a conformational change from parallel to vertical with respect to the plain of the receptor. In the inactive state $Phe^{6.44}$ points between TM V, but in the active model, this amino acid slides between TM III and TM VI, with the consequence that the distance between these two helices is increased (Fig. 4).

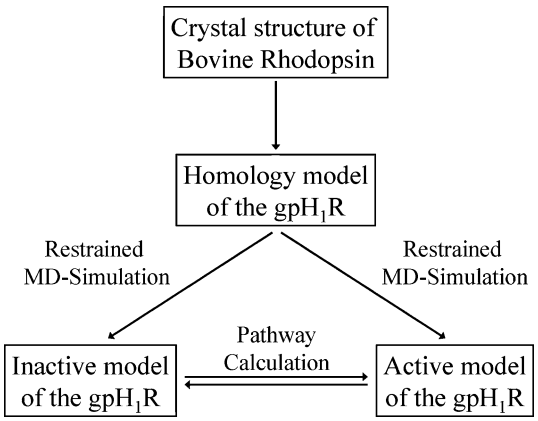

Fig. 1 Flow chart for the modeling of the inactive and active state of the gpH_1R

Changes in interhelical hydrogen bonding and rearrangement of internal water molecules during activation of the gpH_1R

Within our calculations we also observed changes in interhelical hydrogen bonding as given in Table 3. In the

Table 2 Initialization parameters for the different pathway calculations (parameters as described in [35]; the parameters $\Delta\alpha$, $\Delta\beta$, $\Delta\gamma$, n_{TM}, ΔTM_{xy} and $\Delta\theta$ were set to zero because they were not used)

	Activation pathway						Inactivation pathway					
	Run 1	Run 2	Run 3	Run 4	Run 5	Run 6	Run 1	Run 2	Run 3	Run 4	Run 5	Run 6
Seed	56,789	56,789	56,789	56,789	56,789	123	56,789	56,789	56,789	56,789	56,789	123
n	1	4	1	4	1	1	1	4	1	4	1	1
Δr (nm)	0.15	0.15	0.25	0.25	0.25	0.25	0.15	0.15	0.25	0.25	0.25	0.25
$\Delta\varphi$ (°)	5.0	5.0	5.0	5.0	10.0	5.0	5.0	5.0	5.0	5.0	10.0	5.0
$\Delta\rho$ (°)	5.0	5.0	5.0	5.0	5.0	5.0	5.0	5.0	5.0	5.0	5.0	5.0
Δr_{coll} (nm)	0.10	0.10	0.10	0.10	0.10	0.10	0.10	0.10	0.10	0.10	0.10	0.10
$E_0(0)$ (kJ/mol)	−17706	−17706	−17706	−17706	−17706	−17706	−17597	−17597	−17597	−17597	−17597	−17597
$rmsd_0(0)$ (nm)	0.448	0.448	0.448	0.448	0.448	0.448	0.448	0.448	0.448	0.448	0.448	0.448

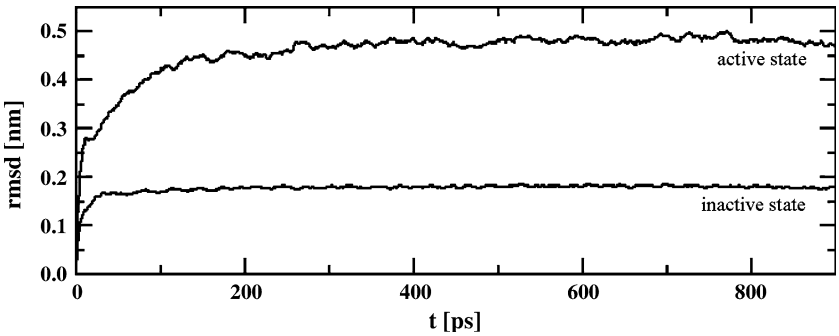

Fig. 2 Time course of rmsd observed during the MD-simulations for generating the inactive and active state model; 0–400 ps: stepwise increase of force constant, 400–800 ps: stepwise decrease of force constant, 800–900 ps: free simulation (a detailed description is given in the part *Modeling of the inactive and active receptor*)

inactive state $Cys^{6.47}$ forms a stable hydrogen bond to the backbone carbonyl moiety of $Leu^{7.41}$. During the activation process this hydrogen bond is broken and $Cys^{6.47}$ forms a hydrogen bond to $Asn^{7.45}$ in the late phase of receptor activation, and establishes a new stable hydrogen bond to the backbone of TM VI in the activated gpH_1R afterwards. $Ser^{3.39}$ forms a stable hydrogen bond to $Asn^{7.45}$ in the inactive state of the gpH_1R (Fig. 5). But because of the counterclockwise rotation of TM III during the activation process this hydrogen bond is lost and $Ser^{3.39}$ moves towards TM II and establishes a hydrogen bond to $Asp^{2.50}$ bridged over one of the internal water molecules (Fig. 5).

Table 3 Stable interhelical hydrogen bonds in the inactive and active gpH_1R (Wat = internal water)

TM–TM-interaction	Inactive gpH_1R	Active gpH_1R
TM I–TM II	$Ser^{1.43}$-$Met^{2.58}$	–
TM I–TM VII	$Thr^{1.46}$-$Thr^{7.47}$, $Asn^{1.50}$-$Ser^{7.46}$	$Thr^{1.46}$-$Thr^{7.47}$, $Asn^{1.50}$-$Ser^{7.46}$
TM II–TM III	$Tyr^{2.42}$-$Ser^{3.42}$, $Tyr^{2.42}$-$Asp^{3.49}$	$Tyr^{2.42}$-$Asp^{3.49}$
TM II–TM IV	$Tyr^{2.42}$-$Thr^{4.45}$	–
TM II–TM VII	$Asn^{2.40}$-$Tyr^{7.53}$	$Asp^{2.50}$-$Ser^{7.46}$, $Asp^{2.50}$-$Asn^{7.49}$
TM III–TM IV	$Thr^{3.37}$-$Ser^{4.53}$	–
TM III–TM V	$Thr^{3.37}$-$Asn^{5.46}$	$Thr^{3.37}$-$Asn^{5.46}$
TM III–TM VI	$Tyr^{3.33}$-$Tyr^{6.51}$	$Tyr^{3.33}$-$Tyr^{6.51}$
TM III–TM VII	$Trp^{3.28}$-$Tyr^{7.43}$, $Ser^{3.39}$-$Asn^{7.45}$	$Asp^{3.32}$-$Tyr^{7.43}$
TM VI–TM VII	$Cys^{6.47}$-$Leu^{7.41}$	–
TM II–internal water	$Asp^{2.50}$-Wat^1, $Asp^{2.50}$-Wat^2, $Ser^{2.61}$-Wat^4	$Leu^{2.46}$-Wat^1, $Asp^{2.50}$-Wat^2, $Ser^{2.61}$-Wat^4
TM III–internal water	–	$Ser^{3.39}$-Wat^2
TM VII–internal water	$Asn^{7.45}$-Wat^3, $Asn^{7.49}$-Wat^2	–
Internal water–internal water	Wat^1-Wat^2	–

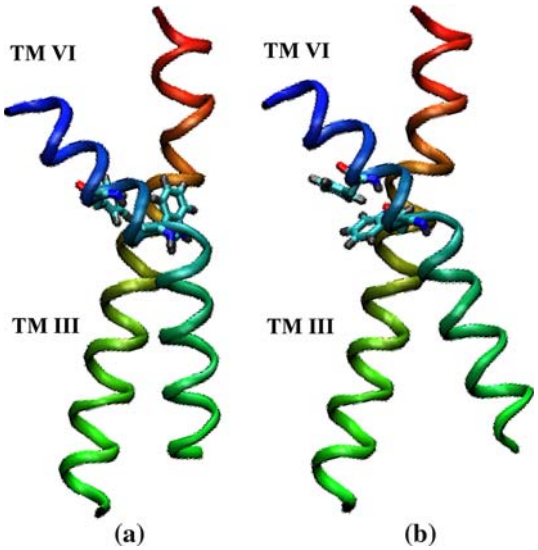

Fig. 3 The aromatic $Trp^{6.48}$/$Phe^{6.52}$-switch and structural change of TM VI in the inactive (**a**) and active (**b**) state of the gpH_1R

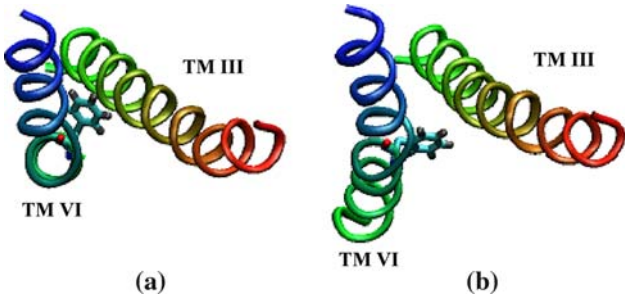

Fig. 4 Conformational change of $Phe^{6.44}$ in the inactive (**a**) and active (**b**) state of the gpH_1R

Jongejan et al. [14] proposed a different hydrogen bonding in the human H_1R (hH_1R) in the intracellular part between TM II, TM III, TM VI and TM VII. In contrast to our calculations they detected a hydrogen bond of $Cys^{6.47}$–$Asn^{7.45}$ in the inactive hH_1R. Additionally they propose a hydrogen bond between $Ser^{3.36}$ and $Asn^{7.45}$ in the inactive state of the hH_1R, which was not detected in our calculations. For $Ser^{3.39}$ they propose a hydrogen bond to $Asn^{7.45}$ in the inactive as well in the active hH_1R. The reason for these differences might be species differences between gpH_1R and hH_1R, the different crystal structures used as template for homology modeling, or the observation of a later activation state in our calculations.

A model for the activation mechanism of the gpH_1R

In Fig. 6a the angle formed by the proline kinked transmembrane helix VI is given. In the inactive state there is an angle of about 135°, which increases up to 150° in the

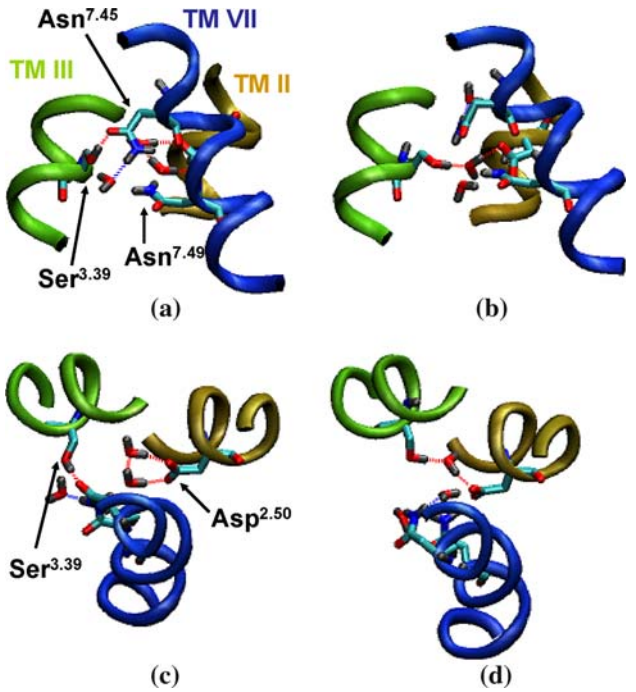

Fig. 5 $Ser^{3.39}$-switch and three conserved internal water molecules between TM II, TM III and TM VII in the intracellular part of the transmembrane helix bundles (**a**) inactive gpH_1R, view from the side, (**b**) active gpH_1R, view from the side, (**c**) inactive gpH_1R, view from the extracellular side, (**d**) active gpH_1R, view from the extracellular side

active state. Accompanied by this linearization of TM VI the distance r between the C_α-atoms of $Arg^{3.50}$ and $Glu^{6.30}$, which form the ionic lock is increased from 0.75 nm up to 1.60 nm. In Fig. 6c the χ_1 rotation angle of $Phe^{6.44}$, $Trp^{6.48}$ and $Phe^{6.52}$ side chains during the activation process are illustrated. In the inactive state the torsion angles (χ_1) of $Phe^{6.52}$ and $Trp^{6.48}$ side chains exhibit a value of about −60°. The χ_1 torsion angle of $Phe^{6.44}$ is about −160° in the inactive conformation. During the activation process up to an *rmsd* of 0.2 nm the absolute value of the torsion angle of $Trp^{6.48}$ is about 10° smaller than for $Phe^{6.52}$. At an *rmsd* of 0.2 nm the torsion angle of $Phe^{6.52}$ does not change any longer, whereas $Trp^{6.48}$ undergoes further conformational changes. Thereby $Phe^{6.52}$ acts as a steric switch for $Trp^{6.48}$ (Fig. 7). The change of the torsion angle of $Trp^{6.48}$ is accompanied by a rotational movement of $Phe^{6.44}$, to avoid a steric clash between these two side chains (Fig. 8). $Phe^{6.44}$ slides between TM III and TM VI (Fig. 4), resulting in an essential increase of the angle formed by the two branches of TM VI, as mentioned above. As a consequence of the reorientation of $Phe^{6.44}$, its side chain comes in close contact to $Ser^{3.39}$ (Fig. 8b, c). Again, to avoid a steric clash between $Phe^{6.44}$ and $Ser^{3.39}$ the serine side chain moves away (Fig. 8c, d), accompanied by a counterclockwise rotation of TM III. During this process the hydrogen bond

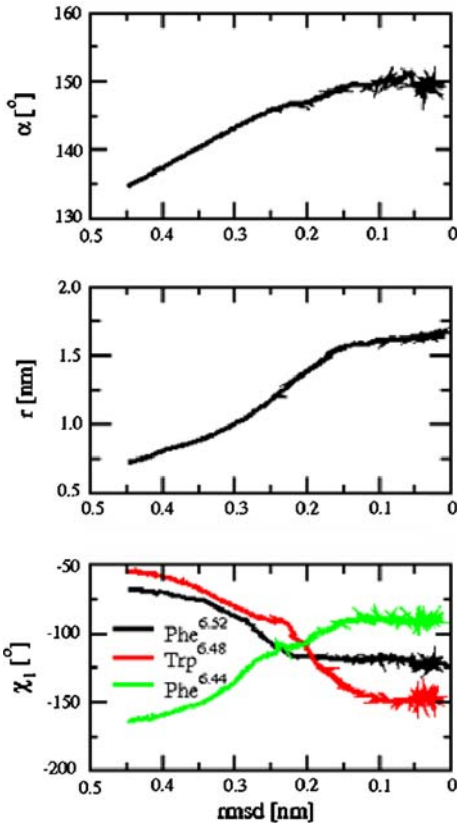

Fig. 6 Structural changes in the gpH_1R during the activation process; on the abscissa the *rmsd* of the inactive state (left) relative to the active state (right) is given; (**a**) angle α formed by the two branches of the proline kinked TM VI, (**b**) distance *r* between the C_α-atoms of $Arg^{3.50}$ and $Glu^{6.30}$ during the activation process of gpH_1R, (**c**) torsion angles χ_1 of $Phe^{6.44}$, $Trp^{6.48}$ and $Phe^{6.52}$

between $Ser^{3.39}$ and $Asn^{7.45}$ is lost (*rmsd* 0.338 nm) and in the later phase of activation (*rmsd* 0.247 nm) the $Ser^{3.39}$ establishes the water-bridged hydrogen bond to $Asp^{2.50}$. A schematic representation of these processes is illustrated in Fig. 9, which contains a 2D projection of the involved amino acids and their movements, as described above.

Figure 10 presents the movement of the transmembrane helices TM I–TM VII during the pathway calculation, characterized by the translation of one helix turn respectively for the extracellular, median and intracellular region. The largest positional changes are observed for TM VI in the intracellular part. Thereby the intracellular distance of TM VI to TM III and TM V increases but decreases between TM VI and TM VII.

Energetical considerations

In Fig. 11 the total of the potential energy of the receptor and the internal water molecules as a function of *rmsd* for the activation and inactivation pathway is given. For this calculation we isolated the receptor and internal water from the whole simulation box (omitting lipid bilayer, extracellular and intracellular water and ions) and carried out a single point energy calculation without further minimization. The starting/destination structures for the inactive and active gpH_1R are indicated by an asterisk. The calculations based on the *LigPath*-algorithm led to an inactive conformation (*rmsd* = 0.42 nm) which more stable than the inactive starting/destination structure, and to an active conformation (*rmsd* = 0.04 nm) which exhibits nearly the same potential energy than the corresponding starting/destination structure. The inactive state (*rmsd* = 0.42 nm) is more stable than the active state (*rmsd* = 0.04 nm). During the activation process the potential energy increases considerably at an *rmsd* of about 0.25 nm with respect to the inactive state. The structures in this area of the potential

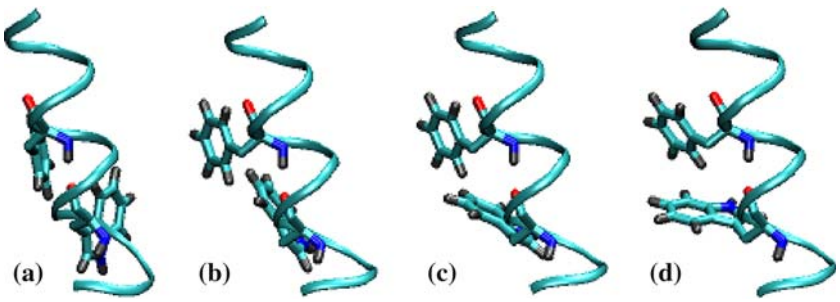

Fig. 7 Conformational changes of $Phe^{6.52}$ and $Trp^{6.48}$ during the activation process (**a**) inactive gpH_1R, (**b**) *rmsd* = 0.219 nm, (**c**) *rmsd* = 0.217 nm, (**d**) active gpH_1R

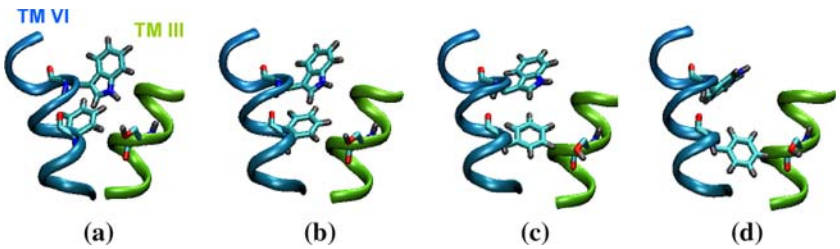

Fig. 8 Snapshots of $Trp^{6.48}$, $Phe^{6.44}$ and $Ser^{3.39}$ during the activation process of gpH_1R (**a**) inactive state (**b**) *rmsd* = 0.338 nm (**c**) *rmsd* = 0.247 nm, (**d**) active state

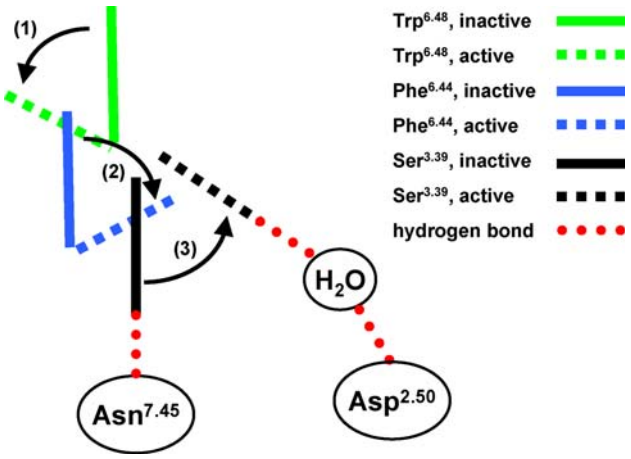

Fig. 9 A 2D model, representing one part of the activation mechanism for the gpH_1R

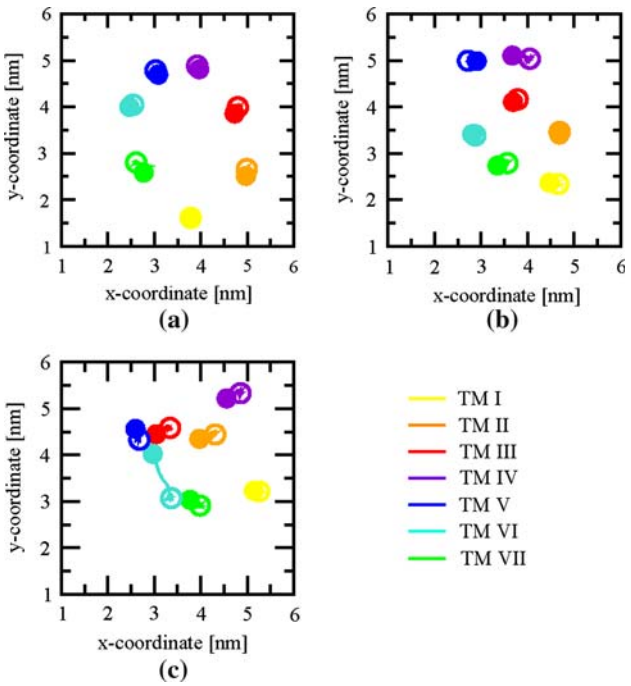

Fig. 10 Movement of the seven transmembrane helices during the activation of the gpH_1R: inactive state (*filled circle*), active state (*non-filled circle*); (**a**) extracellular part, (**b**) median part, (**c**) intracellular part

Table 4 Level of conservation of distinct amino acids

No.	Amino acid	Frequency in amine receptor family (%)	Frequency in histamine receptor family (H_1R–H_4R) (%)	Frequency in H_1R family (%)
1.50	Asn	99.66	100.00	100.00
2.50	Asp	100.00	100.00	100.00
3.25	Cys	99.83	100.00	100.00
3.32	Asp	98.97	100.00	100.00
3.39	Ser	100.00	100.00	100.00
3.49	Asp	98.46	100.00	100.00
3.50	Arg	100.00	100.00	100.00
4.50	Trp	99.66	100.00	100.00
5.47	Phe	98.11	100.00	100.00
5.50	Pro	98.11	100.00	100.00
6.30	Glu	89.54	76.19	100.00
6.44	Phe	98.97	100.00	100.00
6.47	Cys	76.16	100.00	100.00
6.48	Trp	99.14	100.00	100.00
6.50	Pro	99.31	100.00	100.00
6.52	Phe	79.93	76.19	100.00
7.45	Asn	91.94	100.00	100.00
7.46	Ser	98.80	100.00	100.00
7.49	Asn	98.63	100.00	100.00
7.50	Pro	98.80	100.00	100.00
7.53	Tyr	98.11	100.00	100.00

energy surface correlate with the sequence of switches as shown in Figs. 7b, c and 8b, c respectively. In accordance to Fig. 6 the most significant characteristics in activation process are achieved at an *rmsd* of about 0.2 nm, which is reflected in a decrease of potential energy (cf. Fig. 11). For the activation as well as for the inactivation pathway the different runs (Table 2) led to similar energy profiles. The fact, that the differences in energy profiles for the activation and inactivation pathways are distinct can be explained with the large number of degrees of freedom for the receptor atoms. So a single *rmsd* value belongs to perhaps very different receptor conformations, with different potential energies.

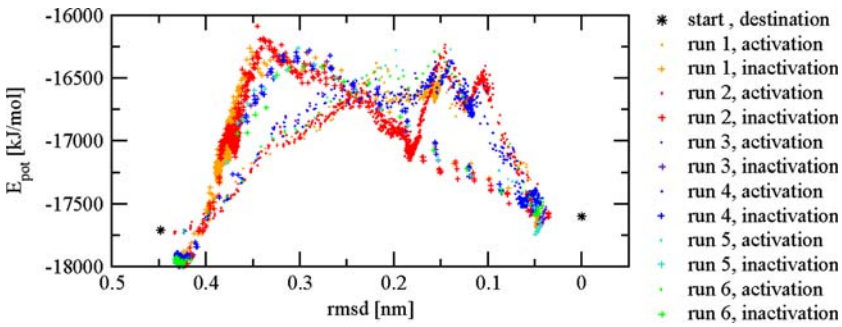

Fig. 11 Energy profile for the activation and inactivation pathway

It should be pointed out, that the values of potential energy must not be taken as absolute values, because of deficiencies in the force field in describing absolute potential energy values. We consider the potential energy profile as indicator to identify specific configurations on potential energy surface qualitatively.

Level of conservation of amino acids involved in receptor activation

In Table 4 an overview concerning the level of conservation of some amino acids is given. This table includes the most conserved amino acids within the amine receptor family of the GPCRs or amino acids which are involved in receptor activation. The data are based on the amine receptors, given in the GPCR database [45] (583 entries). The aromatic switch of $Phe^{6.44}$, $Trp^{6.48}$ and $Phe^{6.52}$ is characteristic for the activation of the gpH_1R, as our calculations have shown. The conservation data (Table 4) show that $Phe^{6.44}$ and $Trp^{6.48}$ occur with a frequency over 98% and $Phe^{6.52}$ with a frequency of about 80%. Also the amino acids $Ser^{3.39}$, $Asn^{7.45}$ and $Asp^{2.50}$ which are involved in the hydrogen bond switch of $Ser^{3.39}$ are highly conserved with more than 90% within the amine and histamine receptor family. So it might be postulated that besides the already known participation of $Trp^{6.48}$ and $Phe^{6.52}$ on receptor activation, also $Phe^{6.44}$, $Ser^{3.39}$ and $Asp^{2.50}$ are not only involved in activation of the gpH_1R but also in activation of other aminergic GPCRs. There are also high levels of conservation for $Asp^{3.32}$ (agonist binding), for $Arg^{3.50}$ and $Glu^{6.30}$ (ionic lock) and for $Pro^{6.50}$ (linearization of the proline kinked TM VI). $Cys^{6.47}$, which is involved in interhelical hydrogen bonding has a conservation level of about 76% within the amine receptor family. For the remaining highly conserved amino acids given in Table 4, we did not found an important influence in activation of the gpH_1R.

Conclusion

With the results of our computations we were able to propose intermediate states during the activation of the gpH_1R and an approximate activation mechanism. The calculations have shown that some highly conserved amino acids might be involved in activation of the gpH_1R, so that it should be possible to transfer the obtained results to other amine receptor subtypes of family A of the GPCRs. To prove or disprove our hypothesis, mutation studies on the gpH_1R could be made, like mutation of $Phe^{6.44}$, $Trp^{6.48}$, $Phe^{6.52}$ and $Ser^{3.39}$. The next step will be a further development of our *LigPath*-algorithm [35], to calculate the pathway of H_1R (partial) agonists or antagonists into their binding-pocket under special consideration of possible receptor activation.

References

1. Evers A, Klabunde T (2005) J Med Chem 48:1088–1097
2. Montero C, Campillo NE, Goya P, Paez JA (2005) Eur J Med Chem 40:75–83
3. Ballesteros JA, Shi L, Javitch JA (2001) Mol Pharmacol 60:1–19
4. Shacham S, Topf M, Avisar N, Glaser F, Marantz Y, Bar-Haim S, Noiman S, Naor Z, Becker OM (2001) Med Res Rev 21:472–483
5. Crocker E, Eilers M, Ahuja S, Hornak V, Hirshfeld A, Sheves M, Smith SO (2006) J Mol Biol 357:163–172
6. Patel AB, Crocker E, Reeves PJ, Getmanova EV, Eilers M, Khorana HG, Smith SO (2005) J Mol Biol 347:803–812
7. Gether U (2000) Endocr Rev 21:90–113
8. Bissantz C (2003) J Recept Signal Transduct 23:123–153
9. Gouldson PR, Kidley NJ, Bywater RP, Psaroudakis G, Brooks HD, Diaz C, Shire D, Reynolds CA (2004) Proteins: Struct. Funct. Bioinf. 56:67–84
10. Singh R, Hurst DP, Barnett-Norris J, Lynch DL, Reggio PH, Guarnieri F (2002) J Pept Res 60:357–370
11. Pardo L, Weinstein H (1997) Int J Quantum Chem 63:767–780
12. Colson A-O, Perlman JH, Jinsi-Parimoo A, Nussenzveig DR, Osman R, Gershengorn MC (1998) Mol Pharmacol 54:968–978
13. Shi L, Liapakis G, Xu R, Guarnieri F, Ballesteros JA, Javitch JA (2002) J Biol Chem 277:40989–40996
14. Jongejan A, Bruysters M, Ballesteros JA, Haaksma E, Bakker RA, Pardo L, Leurs R (2005) Nat Chem Biol 1:98–103
15. Yao X, Parnot C, Deupi X, Ratnala VRP, Swaminath G, Farrens D, Kobilka B (2006) Nat Chem Biol 2:417–422
16. Hallmen C, Wiese M (2006) J Comput Aided Mol Des 20:673–684
17. Barnett-Norris J, Hurst DP, Buehner K, Ballesteros JA, Guarnieri F, Reggio PH (2002) Int J Quantum Chem 88:76–86
18. Urizar E, Claeysen S, Deupi X, Govaerts C, Costagliola S, Vassart G, Pardo L (2005) J Biol Chem 280:17135–17141
19. Behr B, Hoffmann C, Ottolina G, Klotz K-N (2006) J Biol Chem 281:18120–18125
20. Altenbach C, Klein-Seetharaman J, Cai K, Khorana HG, Hubbell WL (2001) Biochemistry 40:15493–15500
21. Farrens DL, Altenbach C, Yang K, Hubbell WL, Khorana HG (1996) Science 274:768–770
22. Ghanouni P, Steenhuis JJ, Farrens DL, Kobilka BK (2001) Proc Natl Acad Sci USA 98:5997–6002
23. Patel AB, Crocker E, Eilers M, Hirshfeld A, Sheves M, Smith SO (2004) Proc Natl Acad Sci USA 101:10048–10053
24. Niv MY, Skrabanek L, Filizola M, Weinstein H (2006) J Comput Aided Mol Des 20:437–448
25. Visiers I, Ebersole BJ, Dracheva S, Ballesteros J, Sealfon SC, Weinstein H (2002) Int J Quantum Chem 88:65–75
26. Reggio PH (2006) AAPS J 8:322–336
27. Fanelli F, de Benedetti PG (2006) J Comput Aided Mol Des 20:449–461
28. Greasley PJ, Fanelli F, Rossier O, Abuin L, Cotecchia S (2002) Mol Pharmacol 61:1025–1032
29. Ballesteros JA, Jensen AD, Liapakis G, Rasmussen SGF, Shi L, Gether U, Javitch JA (2001) J Biol Chem 276:29171–29177
30. Ballesteros J, Kitanovic S, Guarnieri F, Davies P, Fromme BJ, Konvicka K, Chi L, Millar RP, Davidson JS, Weinstein H, Sealfon SC (1998) J Biol Chem 273:10445–10453
31. Huang P, Li J, Chen C, Visiers I, Weinstein H, Liu-Chen L-Y (2001) Biochemistry 40:13501–13509

32. Fanelli F, Menziani C, Scheer A, Cotecchia S, de Benedetti PG (1999) Int J Quantum Chem 73:71–83
33. Pardo L, Deupi X, Dölker N, Lopez-Rodriguez ML, Campillo M (2007) ChemBio Chem 8:19–24
34. Seifert R, Wenzel-Seifert K, Bürckstümmer T, Pertz HH, Schunack W, Dove S, Buschauer A, Elz S (2003) J Pharmacol Exp Ther 305:1104–1115
35. Straßer A, Wittmann H-J (2007) J Mol Model 13:209–218
36. SYBYL 7.0 (2004) Tripos Inc. (Software)
37. VEGA ZZ, Pedretti A, Vistoli G (1996–2006) (Software) http://www.ddl.unimi.it/vega
38. RCSB PDB Protein Data Bank
39. Palczewski K, Kumasaka T, Hori T, Behnke CA, Motoshima H, Fox BA, Le Trong I, Teller DC, Okada T, Stenkamp RE, Yamamoto M, Miyano M (2000) Science 289:739–745
40. Li J, Edwards PC, Burghammer M, Villa C, Schertler GF (2004) J Mol Biol 343:1409–1438
41. van der Spoel D, Lindahl E, Hess B, van Buuren AR, Apol E, Meulenhoff PJ, Tieleman DP, Sijbers ALTM, Feenstra KA, van Drunen R, Berendsen HJC (2004) GROMACS 3.2. Department of Biophysical Chemistry, University of Groningen, The Netherlands
42. Oostenbrink C, Villa A, Mark AE, van Gunsteren WF (2004) J Comput Chem 25:1656–1676
43. vmd for LINUX version 1.8.4 (2006) (Software) http://www.ks.uiuc.edu/Research/vmd
44. Humphrey W, Dalka A, Schulten K (1996) J Mol Graph 14:33–38
45. GPCR Database (January 2007) http://www.gpcr.org/7tm/seq/